Quantum Hall ice

Gia-Wei Chern, Armin Rahmani, Ivar Martin, and Cristian D. Batista

Phys. Rev. B **90**, 241102 — Published 1 December 2014

DOI: 10.1103/PhysRevB.90.241102

Quantum Hall Ice

Gia-Wei Chern,[1] Armin Rahmani,[1] Ivar Martin,[1] and Cristian D. Batista[1]

[1] *Theoretical Division, T-4 and CNLS, Los Alamos National Laboratory, Los Alamos, NM 87545, USA*

(Dated: November 18, 2014)

We show that the chiral kagome ice manifold exhibits an anomalous integer quantum Hall effect (IQHE) when coupled to itinerant electrons. Although electron-mediated interactions select a magnetically ordered ground state, the full ice manifold can coexist with the IQHE over a range of finite temperatures. The degenerate ice states provide a natural realization of power-law correlated flux disorder, for which the spectral gap of the system remains robust. The quantized (up to exponentially small finite-temperature corrections) Hall conductance persists over a wide range of electron densities due to the disorder-induced localization of electronic states.

PACS numbers: 71.10.Fd, 73.43.-f,75.10.Hk

The integer quantum Hall effect (IQHE) is characterized by a topological invariant known as the first Chern number[1]. Besides the well-known two-dimensional (2D) electron gas in a magnetic field, quantum Hall effect can also emerge spontaneously from the interplay of itinerant electrons and local magnetic moments in the absence of an external magnetic field[2,3]. The origin of this phenomenon lies in the Berry phases imparted to the electrons by magnetic textures with finite scalar spin chirality $\chi_{ijk} = \mathbf{S}_i \cdot \mathbf{S}_j \times \mathbf{S}_k$. Such quantized Hall conductance can certainly be generated through long-range noncoplanar magnetic ordering: $\langle \mathbf{S}_j \rangle, \langle \chi_{ijk} \rangle \neq 0$[4–11]. Notably, the scalar spin chirality can exist even without long-range magnetic order: $\langle \mathbf{S}_j \rangle = 0$ and $\langle \chi_{ijk} \rangle \neq 0$[7,8]. Indeed, for 2D systems, the chiral ordered phase can persist at finite temperatures (it only breaks a discrete Z_2 symmetry), while magnetic order is destroyed by thermal fluctuations.[12]

The stability of the Hall conductance in such itinerant magnets is due to a robust locally ordered non-coplanar structure. While spin waves destroy the long-range magnetic order at finite temperature (T), long-wavelength distortions of the spin texture do not change the Berry flux pattern[7]. A quantized Hall liquid, however, can also be stabilized in a state with strongly disordered Berry fluxes, as we demonstrate for a geometrically frustrated itinerant magnet. Up to exponentially small finite-T corrections, an IQHE can coexist with an extensively degenerate ice manifold of magnetic local moments in a kagome lattice. This "quantum Hall ice" phase is a proof of principle for a new state of matter: an integer quantum Hall liquid coexisting with a classical spin ice. This work is partly motivated by recent experiments on a metallic spin-ice compound $Pr_2Ir_2O_7$, which shows an anomalous Hall effect in the absence of any magnetic ordering[13–15].

We show here that itinerant magnets with geometrical frustration provide experimentally relevant examples of correlated non-Gaussian disorder, which could have profound effects on the electronic states (such peculiar spin correlations, e.g., can explain the resistivity minimum of metallic spin ice[16,17]). Despite great theoretical interest in the effects of correlated disorder on electron transport, experimental realizations have remained elusive[18–21]. Moreover, non-Gaussian disorder is expected to give rise to novel phenomena[22] but rarely appears in nature (disorder from impurities in general have an uncorrelated Gaussian distribution).

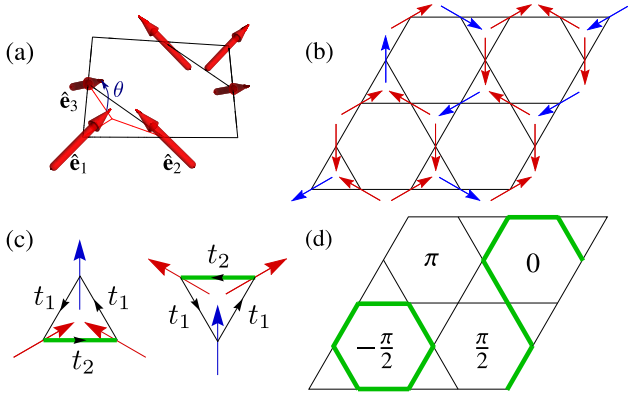

FIG. 1: (a) The kagome lattice and the Ising axes $\hat{\mathbf{e}}_i$ for local magnetic moments $\mathbf{S}_i = \sigma_i \hat{\mathbf{e}}_i$. (b) The projection of $\mathbf{S}_i$ on the plane of the lattice for a random chiral kagome-ice configuration. Spins with $\sigma = +1$ ($\sigma = -1$) are shown in red (blue). (c) Two types of hopping amplitudes in a large-J spinless effective model. (d) The fluxes in the effective model through the hexagonal plaquettes for the ice configuration of panel (b) at the special canting angle θ^*.

One special feature of the peculiar power-law correlated flux disorder, originating from the ice rules, is the robustness of the spectral gap. Although amorphous solids are known to exhibit spectral gaps for strong disorder, survival of a spectral gap is unprecedented for strongly disordered IQHLs[23]. Another interesting feature concerns the properties of the magnetic monopoles (plaquettes that violate ice rules). Topological defects in itinerant magnets are known to exhibit unusual phenomena such as charge fractionalization[24]. Here we demonstrate that pinned magnetic monopoles[25,26] in the quantum Hall ice induce a fluctuating electric dipole in the charge density of the itinerant electrons.

We consider a kagome-lattice model in which Ising-like spins are subject to local constraints resembling the Bernal-Fowler ice rules[27]. This so-called "kagome ice"[28] is an easy-axis ferromagnet with spins sitting on a two-dimensional network of corner-sharing triangles (Fig. 1). The projections of the local easy axes $\hat{\mathbf{e}}_i$ on the kagome plane form a 120-degree ordering, while the axes are canted with respect to this plane by an angle θ. The spin direction is specified by a set of Ising variables σ_i as $\mathbf{S}_i = \sigma_i \hat{\mathbf{e}}_i$. The magnetic charges (in natural

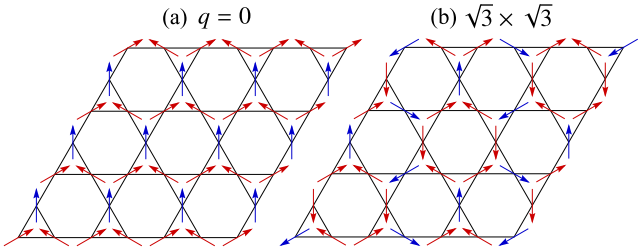

FIG. 2: (Color online) (a) The $q = 0$ ice state. (b) The $\sqrt{3} \times \sqrt{3}$ ice state.

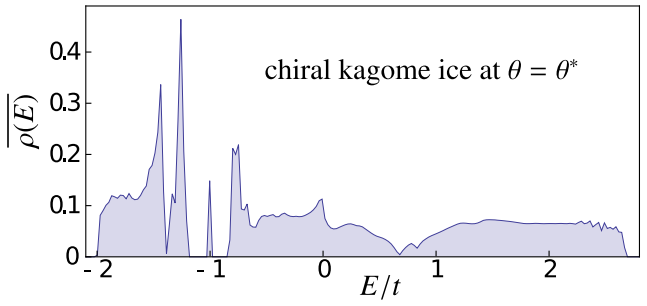

FIG. 3: (Color online) The disorder-averaged density of states $\overline{\rho(E)}$ for chiral kagome ice at $\theta = \theta^*$.

units) for every up and down triangles are $Q_\triangle = -\sum_{i\in\triangle}\sigma_i$ and $Q_\triangledown = +\sum_{i\in\triangledown}\sigma_i$. The nearest-neighbor ferromagnetic exchange between spins $\mathbf{S}_i$ can be recast into $\sum_\alpha Q_\alpha^2$[28,29], which penalizes triangles with magnetic charge ± 3. It is thus energetically favorable for each triangle to have magnetic charges ± 1. This implies the constraint that every triangle has either two incoming and one outgoing spins or vice versa.

A subset of this kagome-ice manifold, known as the charge-ordered or *chiral* kagome ice[29,30], has a further constraint that spins in every up (down) triangle must be 2-in-1-out (1-in-2-out), i.e. all $Q_\triangle = -1$ and all $Q_\triangledown = +1$[29,30]. Such configurations may be stabilized by two-body interactions of the form $Q_\triangle Q_\triangledown$, long-range dipolar interactions[29,30], or alternatively in spin-ice pyrochlores subject to a magnetic field in the [111] direction[31,32] (in the presence of itinerant electrons, the 3D pyrochlore lattice may be approximated by decoupled 2D kagome layers if the inter-layer hopping is weak). Furthermore, it may be possible to stabilize chiral kagome ice through the electron-mediated interactions themselves.

Although there is no long-range order in the Ising variables σ_i, the chiral kagome ice does have an overall magnetization in the out-of-plane direction, and our results do not directly explain the experiments on $Pr_2Ir_2O_7$, where the anomalous quantum Hall effect seems to persist even in the absence of net magnetization. Motivated by $Pr_2Ir_2O_7$, however, the chiral itinerant kagome ice in a magnetic field was studied recently in the limit of low densities and small Kondo coupling, where an anomalous (nonquantized) Hall response was obtained[33]. Here we focus on the opposite limit of large Kondo coupling and finite densities in a broad range close 1/3 filling and find a quantized response.

We now introduce the itinerant electrons, which are coupled to the above Ising-like moments on the kagome lattice via an exchange coupling J. The electronic part of the Hamiltonian is then given by

$$H = t\sum_{\alpha\langle ij\rangle}\left(c^\dagger_{i\alpha}c_{j\alpha} + \text{H.c.}\right) + J\sum_{i\alpha\beta}\mathbf{S}_i\cdot c^\dagger_{i\alpha}\boldsymbol{\sigma}_{\alpha\beta}c_{i\beta}, \qquad (1)$$

where $c_{i\alpha}$ is a fermionic annihilation operator on site i and spin α and t is the hopping amplitude. If the classical energy scales are much larger than the electron-mediated spin-spin interactions, the coupling to itinerant electrons does not bring the system out of the ice manifold. Before a discussion of the energetics, we examine the fate of the electronic state for each chiral kagome-ice configuration of local moments $\mathbf{S}_i$.

To examine the intrinsic topological properties of the electrons in this ice manifold, we further simplify the problem by first considering the strong coupling limit. In the $|J| \gg |t|$ limit, the electrons align themselves with the local moments and the effective hopping amplitude between two sites with local moments $\mathbf{S}_i$ and $\mathbf{S}_j$ becomes $t\langle\chi_i|\chi_j\rangle$, where $|\chi_i\rangle$ is the spinor eigenstate of $\mathbf{S}_i\cdot\boldsymbol{\sigma}_{\alpha\beta}$. As shown in Fig. 1(c), there are two distinct hopping constants: $t_1 = \cos\frac{\pi}{6}e^{-i\frac{\pi}{6}}\cos\theta$ and $t_2 = \sin\frac{\pi}{6}e^{i\frac{\pi}{3}} + \cos\frac{\pi}{6}e^{-i\frac{\pi}{6}}\sin\theta$, for opposite and same Ising spins on the bond, respectively. The gauge-invariant fluxes, which determine the electronic properties, can be obtained from the above (gauge-dependent) amplitudes. These fluxes are equal in all up and down triangular plaquettes:

$$\Phi_\triangle = \Phi_\triangledown = 2\phi_1 + \phi_2, \qquad \phi_i \equiv \arg(t_i). \qquad (2)$$

The fluxes in the hexagonal plaquettes of a generic chiral ice state, on the other hand, depend on the ice configuration, giving rise to a model of flux disorder. These hexagonal fluxes are not uncorrelated. To see this, let us write the flux in a hexagon in terms of the six Ising variables around a hexagon as follows:

$$\Phi_\hexagon = -6\phi_1 + (\phi_1 - \phi_2)\sum_{i\in\hexagon}\sigma_i, \qquad (3)$$

where $\sum_{i\in\hexagon}\sigma_i$ can take four distinct values: 0, 2, 4, and 6. Due to a mapping of the chiral ice manifold to a dimer model on the honeycomb lattice[32,34], the Ising spins and consequently the fluxes above exhibit power-law correlations

$$\overline{\Phi_\hexagon(\mathbf{r})\Phi_\hexagon(0)} - \left(\overline{\Phi_\hexagon(\mathbf{r})}\right)^2 \sim 1/r^2, \qquad (4)$$

where the "overline" indicates an average over chiral kagome ice configurations (see the Supplemental Material for details). Note that the average flux in a hexagonal plaquette $\langle\Phi_\hexagon(\mathbf{r})\rangle = -4\phi_1 - 2\phi_2$, is generically nonzero (the total flux through all triangles and hexagons vanishes). The same mapping to dimers also suggests that the flux disorder above is non-Gaussian.

The magnitude of the hopping amplitudes can, in general, take two different values $|t_1|$ and $|t_2|$. At a special canting angle $\theta = \theta^* = \frac{1}{2}\arccos\left(\frac{1}{3}\right)$, which we mostly focus on in the present paper, we have $|t_1| = |t_2| = \frac{t}{\sqrt{2}} \equiv \tilde{t}$. For this special θ, the phases of the hopping amplitudes are given by $\phi_1 = -\frac{\pi}{6}$

and $\phi_2 = \frac{\pi}{12}$, which according to Eqs. (2) and (3) leads to a flux $-\frac{\pi}{4}$ in every triangular plaquette, and four different fluxes in the hexagonal ones, as shown in Fig. 1(d).

In an ordered $q = 0$ configuration [see Fig. 1(a)], which belongs to the chiral ice manifold, the flux in all hexagons is equal to $-2\Phi_\triangle$. The tight-binding Hamiltonian is known to exhibit a spectral gap and an IQHE at $1/3$ and $2/3$ filling fractions for this orderd state[4]. The topological origin of the quantum Hall effect in the $q = 0$ state can be understood by considering its band structure in the limits of $\theta = 0$ and $\theta = \frac{\pi}{2}$. The fluxes vanish in all plaquettes at $\theta = 0$ but the tight-binding spectrum has pairs of Dirac points at 1/3 and 2/3 filling fractions. Non-zero fluxes resulting from canted spins gap out the Dirac points and lead to nontrivial band Chern numbers[2,4]. In the $\theta = \frac{\pi}{2}$ limit, on the other hand, we obtain an array of one-dimensional chains. Moving away from $\theta = \frac{\pi}{2}$ results in coupling these noninteracting Luttinger liquids (in the presence of time-reversal-symmetry-breaking fluxes), which also leads to quantum Hall effect[35,36].

For random chiral ice states, the electrons experience flux disorder according to Eqs. (3) and (4). Generically, flux disorder should not differ from electrostatic potential disorder if there is a net flux through the system[37]. In case of the chiral kagome ice, the average flux vanishes, but since the system is characterized by a global quantum Hall response, one expects similar behavior to quantum Hall systems, which emerge in the presence of a net magnetic field. Generically, strong disorder closes the spectral gap in integer quantum Hall liquids (see, e.g., Ref.[23]) but the quantum Hall effect nevertheless persists at $T = 0$. This can be understood in terms of a critical point (localization-delocalization transition) between two insulating states with extended states appearing only at a single critical energy E_c[38–41]. For the peculiar power-law correlated disorder considered here, we find that not only does the quantized Hall conductance remain robust, but also the spectral gap at 1/3 filling remarkably persists even in the presence of strong flux disorder.

Fig. 3(a) shows the disorder-averaged density of states obtained using loop-update Monte Carlo simulations at the special canting angle θ^*. A spectral gap $\Delta \sim 0.2t$ can be clearly seen. Interestingly, we also observe a peak in the middle of the spectral gap. This peak corresponds to a flat band[42] of localized states around hexagonal plaquettes with $\Phi_\bigcirc = -\pi/2$. We have checked that the spectral gap and a quantized Hall conductance in the kagome ice manifold remain robust for a broad range of canting angles, which include θ^* (see also Ref.[43] for a detailed study). The ice rules are indeed important for the robustness of the spectral gap. As shown in the Supplemental Material, both continuous and discrete uncorrelated random fluxes close the gap.

We computed the above-mentioned quantum Hall conductance σ_{xy} explicitly for each ice configuration using the real-space version of the Kubo formula $\sigma_{xy} = \sum'_m \sigma^m_{xy}$, where $\sum'$ indicates summation over occupied levels m, and

$$\sigma^m_{xy} = \frac{2e^2\hbar}{A} \sum_{n\neq m} \mathrm{Im}\left[\frac{\langle m|v_x|n\rangle\langle n|v_y|m\rangle}{(E_m - E_n)^2}\right], \qquad (5)$$

where $|n\rangle$ is a single-particle eigenstate with energy E_n, A is the area of the system, and v_i is the velocity operator in direction $i = x, y$. We found that σ_{xy} is indeed quantized at filling fractions $1/3$ and $2/3$ for all chiral kagome ice configurations.

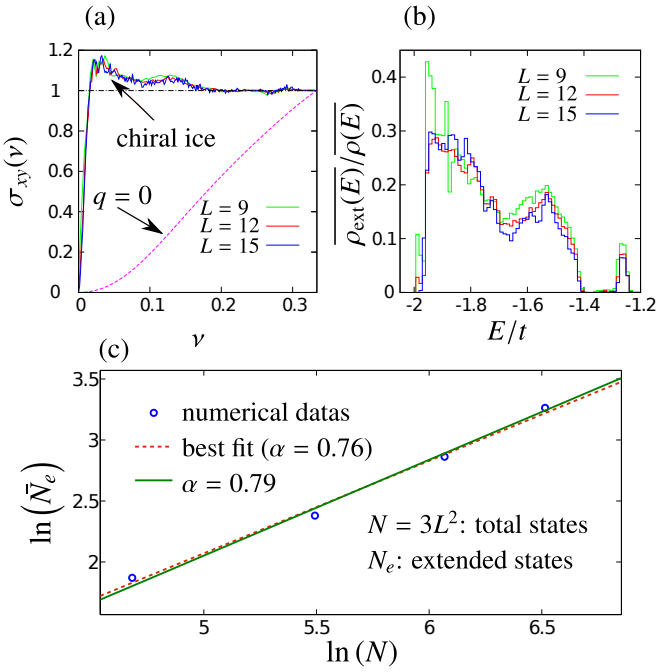

FIG. 4: (Color online) (a) The disorder-averaged Hall conductance as a function of the Fermi energy. (b) The ratio of density of extended states to the total density of states. (c) The number of extended states as a function of the the system size.

Fig. 4(a) shows the σ_{xy} as a function of the filling fraction ν for the $q = 0$ state as well as the disorder-averaged σ_{xy} for the full chiral kagome ice manifold. In order to suppress finite-size effects in the above calculation of $\sigma_{xy}(\nu)$, we average σ^m_{xy} [Eq. (5)] over various boundary phases, where a phase 0 (π), e.g., corresponds to periodic (antiperiodic) boundary conditions. The Hall conductance rises much more quickly when increasing the density for chiral kagome ice than the clean $q = 0$ ice state, and approaches its quantized value at a significantly smaller ν. Similar to traditional quantum Hall states, where disorder leads to plateaus of transverse conductance as a function of the filling fraction, disorder stabilizes a $T = 0$ quantized conductance over a wide range of filling fractions in chiral kagome ice.

The localization properties of the system can be explored in more detail by identifying localized and extended single-particle states. For each realization of the disorder, the angle-averaged $\langle\sigma^m_{xy}\rangle$ is an integral multiple of e^2/h[23,44–48]. A state $|m\rangle$ with nonzero $\langle\sigma^m_{xy}\rangle \neq 0$ carries Hall current and is necessarily an extended state[45]. This allows us to compute the average density of extended states. Fig. 4(b) shows the ratio of extended to total density of states. While the two higher energy peaks in Fig. 4(b) decrease with increasing the system size, the lowest-energy peak persists and roughly coincides with the abrupt rise of $\overline{\sigma_{xy}}$ in Fig. 4(a). We estimate a critical energy $E_c = (1.9 \pm 0.1)t$, close to the bottom of the band. This is in contrast to the traditional quantum Hall liquids, in which

extended states appear in the middle of the broadened Landau level (the gap generally vanishes as Landau levels overlap). The proximity of E_c to the bottom of the band explains why the Hall conductivity rises up quickly to its quantized value in chiral kagome ice.

At the critical energy, E_c, the localization length is expected to diverge as $|E-E_c|^{-\nu}$ (the exponent ν not to be confused with the filling fraction). For Gaussian power-law correlated disorder with an exponent 2, as in Eq. (4), we expect this critical point to have an exponent $\nu = 2.33$[20,21]. We have checked the exponents for our non-Gaussian case by comparing the number of extended states N_e (averaged over the kagome ice manifold) at a given system size with the total number of states N, which should go as N^α, with $\alpha = 1 - 1/2\nu$. As shown in Fig. 4(c), the results indicate that the localization exponent is approximately equal to $\nu = 2.33$, as in the case of Gaussian disorder.

We now address the energetics of the system in detail. So far, we assumed that the chiral kagome ice was stabilized by certain interactions between local moments and added the electrons in an *ad hoc* manner. To study the energetic stability of this phase, we performed classical Monte Carlo simulations for large J/t, $\nu = 1/3$ and $\theta = \theta^*$ and found that in fact at $T = 0$, the $q = 0$ [Fig. 2(a)] state has the lowest energy. However, this state is not a unique ground state: assuming periodic boundary conditions, we can transform the $q = 0$ state to other ice states, with the same flux pattern, by flipping loops of spins. Similarly, the highest-energy state appears to be the $\sqrt{3}\times\sqrt{3}$ [Fig. 2(b)] state and related degenerate states, which give rise to the same flux pattern.

As shown in Fig. 2, all chiral ice configurations give rise to a single-particle spectral gap Δ at $1/3$ filling fraction, which is typically an order of magnitude larger than the difference, δ, between the energy densities (per lattice site) of the $q = 0$ and $\sqrt{3}\times\sqrt{3}$ configurations. (At $\theta = \theta^*$ and $1/3$ filling, we have $\delta = 0.02t$ and $\Delta = 0.12t$.) Since δ serves as a characteristic energy scale for electron-mediated spin-spin interactions, the energy difference between different chiral ice configurations is not resolved at temperatures $\delta \ll T \ll \min_{\{\sigma\}} \Delta(\{\sigma\})$, while the corrections to the quantized σ_{xy} are exponentially small in the Δ/T ratio over such range of temperatures.

After establishing the existence of the quantum Hall ice phase and studying its (bulk) topological and localization properties, we consider the interplay of magnetic monopoles with itinerant electrons in this system. Indeed, one of the most fascinating properties of spin ice is the emergent magnetic monopoles. These emergent excitations are defects violating the local ice constraints, which in the case of chiral kagome ice require $Q_\triangle = -1$ and $Q_\triangledown = 1$. Emergent magnetic monopoles in the chiral ice are triangles with $Q_\triangle = 1$ and $Q_\triangledown = -1$[49] (we neglect the higher-energy defects with $Q_{\triangle,\triangledown} = \pm 3$).

In a given ice configuration, flipping an open string of head-to-tail spins can create two such triangles, which violate the ice rules. The defects in turn change the Berry flux pattern experienced by the electrons (see Supplemental Material for details). Interestingly, an incarnation of Laughlin's flux-insertion argument in this quantum Hall state predicts the formation electric dipoles pointing from the center of the (monopole) triangle to the center of the neigboring hexagons. Detection of such dipoles in a given realization is difficult because the charge density is not generically uniform, and flipping a finite string creates charge density variations with a similar magnitude to the variations already present in a typical configuration.

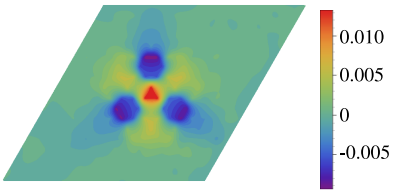

FIG. 5: Numerically computed charge density in the vicinity of a pinned magnetic monopole, averaged over ice realizations with two monopole defects (the shown region has 24×24 lattice spacings).

However, magnetic monopoles, which are in fact defined for the full fluctuating spin ice manifold, can be pinned by impurities. For two such pinned monopoles, the charge density profile is uniform away from the defects after averaging over a time scale longer than the characteristic time scales of the spin dynamics. The remnants of the above-mentioned electric dipoles appear around each monopole as three electric dipoles with C_3 symmetry (see Fig. 5).

In summary, the magnetic exchange between conduction electrons and a frustrated set of local Ising moments can lead to a novel state matter, simultaneously characterized by spin-ice local moment physics and a quantized (with exponentially small finite-T corrections) anomalous quantum Hall effect for itinerant electrons over a wide range of filling factors. This spontaneously broken symmetry state does not require of any external magnetic field or spin-orbit interaction. The critical correlations of spin ice produce a peculiar form of power-law correlated flux disorder that has nontrivial consequences on the spectrum and transport properties of the conduction electrons. While previous studies have focused on the longitudinal conductivity of "metallic-ice"[16,17], we have shown that *chiral* spin-ice can dramatically change the electronic state by inducing a robust Quantum Hall liquid ("Quantum Hall ice"). Moreover, the interplay of the electrons with magnetic monopole defects may provide novel electronic signatures for detecting these monopoles.

Acknowledgments

We are grateful to C. Castelnovo, S. Trugman, and K. Yang for helpful discussions. This work was supported by the U.S. DOE under LANL/LDRD program (C.B., G.W.C., I.M., and A.R.) and a LANL Oppenheimer fellowship (G.W.C.). Upon completion of this work, we became aware of an independent parallel work[50], in which the quantum Hall ice phase was also predicted in full agreement with our findings. Beyond this fundamental result, these two related works address different aspects of the problem (e.g., localization and topological de-

fects in the present manuscript).

[1] D. J. Thouless, M. Kohmoto, M. P. Nightingale, and M. den Nijs, Phys. Rev. Lett. **49**, 405 (1982).
[2] F. D. M. Haldane, Phys. Rev. Lett. **61**, 2015 (1988).
[3] Y. Taguchi, Y. Oohara, H. Yoshizawa, N. Nagaosa, and Y. Tokura, Science **30**, 2573 (2001).
[4] K. Ohgushi, S. Murakami, and N. Nagaosa, Phys. Rev. B **62**, R6065 (2000).
[5] R. Shindou and N. Nagaosa, Phys. Rev. Lett. **87**, 116801 (2001).
[6] Y. Akagi and Y. Motome, J. Phys. Soc. Jpn. **79**, 083711 (2010).
[7] I. Martin and C. D. Batista, Phys. Rev. Lett. **101**, 156402 (2008).
[8] I. Martin and C. D. Batista, Phys. Rev. Lett. **105**, 266405 (2010).
[9] T. Li, Europhys. Lett. **97**, 37001 (2012).
[10] S.-L. Yu and J.-X. Li, Phys. Rev. B **85**, 144402 (2012).
[11] J. W. F. Venderbos, M. Daghofer, J. van den Brink, and S. Kumar, Phys. Rev. Lett. **109**, 166405 (2012).
[12] N. D. Mermin and H. Wagner, Phys. Rev. Lett. **17**, 1133 (1966), URL `http://link.aps.org/doi/10.1103/PhysRevLett.17.1133`.
[13] S. Nakatsuji, Y. Machida, Y. Maeno, T. Tayama, T. Sakakibara, J. v. Duijn, L. Balicas, J. N. Millican, R. T. Macaluso, and J. Y. Chan, Phys. Rev. Lett. **96**, 087204 (2006).
[14] Y. Machida, S. Nakatsuji, Y. Maeno, T. Tayama, T. Sakakibara, and S. Onoda, Phys. Rev. Lett. **98**, 057203 (2007).
[15] Y. Machida, S. Nakatsuji, S. Onoda, T. Tayama, and T. Sakakibara, Nature **463**, 210 (2009).
[16] M. Udagawa, H. Ishizuka, and Y. Motome, Phys. Rev. Lett. **108**, 066406 (2012).
[17] G.-W. Chern, S. Maiti, R. M. Fernandes, and P. Wölfle, arXiv:1210.3289 (2012).
[18] J. M. Ziman, Phil. Mag. **6**, 1013 (1961).
[19] M. E. Fisher and J. S. Langer, Phys. Rev. Lett. **20**, 665 (1968).
[20] N. Sandler, H. R. Maei, and J. Kondev, Phys. Rev. B **70**, 045309 (2004).
[21] B. Huckestein, Rev. Mod. Phys. **67**, 357 (1995).
[22] H. Javan Mard, E. C. Andrade, E. Miranda, and V. Dobrosavljevi, arXiv:1309.0475 (2013).
[23] K. Yang and R. N. Bhatt, Phys. Rev. Lett. **76**, 1316 (1996).
[24] A. Rahmani, R. A. Muniz, and I. Martin, Phys. Rev. X **3**, 031008 (2013).
[25] I. A. Ryzhkin, JETP **101**, 481 (2005).
[26] C. Castelnovo, R. Moessner, and S. L. Sondhi, Nature **451**, 42 (2008).
[27] S. T. Bramwell and M. J. P. Gingras, Science **294**, 14951501 (2001).
[28] A. S. Wills, R. Ballou, and C. Lacroix, Phys. Rev. B **66**, 144407 (2002).
[29] G.-W. Chern, P. Mellado, and O. Tchernyshyov, Phys. Rev. Lett. **106**, 207202 (2011).
[30] G. Möller and R. Moessner, Phys. Rev. B **80**, 140409 (2009).
[31] K. Matsuhira, Z. Hiroi, T. Tayama, S. Takagi, and T. Sakakibara, Journal of Physics: Condensed Matter **14**, L559 (2002).
[32] M. Udagawa, M. Ogata, and Z. Hiroi, J. Phys. Soc. Jpn. **71**, 2365 (2002).
[33] M. Udagawa and R. Moessner, Phys. Rev. Lett. **111**, 036602 (2013).
[34] R. Moessner and S. Sondhi, Phys. Rev. B **68**, 064411 (2003).
[35] S. L. Sondhi and K. Yang, Phys. Rev. B **63**, 054430 (2001).
[36] C. L. Kane, R. Mukhopadhyay, and T. C. Lubensky, Phys. Rev. Lett. **88**, 036401 (2002).
[37] V. Kalmeyer, D. Wei, D. P. Arovas, and S. Zhang, Phys. Rev. B **48**, 11095 (1993).
[38] S. Trugman, Phys. Rev. B **27**, 7539 (1983).
[39] J. T. Chalker and P. D. Coddington, J. Phys. C: Solid State Phys. **21**, 2665 (1988).
[40] B. Huckestein and B. Kramer, Phys. Rev. Lett. **64**, 1437 (1990).
[41] Y. Huo and R. N. Bhatt, Phys. Rev. Lett. **68**, 1375 (1992).
[42] M. Udagawa, H. Ishizuka, and Y. Motome, arXiv:1310.4580 (2013).
[43] H. Ishizuka and Y. Motome, arXiv:1309.4901 (2013).
[44] D. J. Thouless, J. Phys. C **17**, L325 (1984).
[45] D. P. Arovas, R. N. Bhatt, F. D. M. Haldane, P. B. Littlewood, and R. Rammal, Phys. Rev. Lett. **60**, 619 (1988).
[46] K. Yang and R. N. Bhatt, Phys. Rev. B **55**, R1922 (1997).
[47] K. Yang and R. N. Bhatt, Phys. Rev. B **59**, 8144 (1999).
[48] D. N. Sheng and Z. Y. Weng, Phys. Rev. Lett. **75**, 2388 (1995).
[49] E. Mengotti, L. J. Heyderman, A. F. Rodriguez, F. Nolting, R. V. Hugli, and H.-B. Braun, Nat. Phys. **7**, 68 (2011).
[50] H. Ishizuka and Y. Motome, arXiv:1212.3855 (2013).